

OPEN ACCESS

EDITED BY

Bertrand Kibler,
UMR6303 Laboratoire Interdisciplinaire Carnot
de Bourgogne (ICB), France

REVIEWED BY

Vin-Cent Su,
National United University, Taiwan
Yijie Shen,
Nanyang Technological University, Singapore

*CORRESPONDENCE

Gianluca Ruffato,
✉ gianluca.ruffato@unipd.it

RECEIVED 02 February 2024

ACCEPTED 04 April 2024

PUBLISHED 07 May 2024

CITATION

Vogliardi A, Bonaldo D, Dal Zilio S, Romanato F
and Ruffato G (2024), Design, fabrication, and
test of bi-functional metalenses for the spin-
dependent OAM shift of optical vortices.
Front. Phys. 12:1381156.
doi: 10.3389/fphy.2024.1381156

COPYRIGHT

© 2024 Vogliardi, Bonaldo, Dal Zilio, Romanato
and Ruffato. This is an open-access article
distributed under the terms of the [Creative
Commons Attribution License \(CC BY\)](#). The use,
distribution or reproduction in other forums is
permitted, provided the original author(s) and
the copyright owner(s) are credited and that the
original publication in this journal is cited, in
accordance with accepted academic practice.
No use, distribution or reproduction is
permitted which does not comply with
these terms.

Design, fabrication, and test of bi-functional metalenses for the spin-dependent OAM shift of optical vortices

Andrea Vogliardi^{1,2}, Daniele Bonaldo^{2,3}, Simone Dal Zilio⁴,
Filippo Romanato^{1,2,4} and Gianluca Ruffato^{1,2,3*}

¹Department of Physics and Astronomy "G. Galilei", University of Padova, Padova, Italy, ²Padua Quantum Technologies Research Center, University of Padova, Padova, Italy, ³Department of Information Engineering, University of Padova, Padova, Italy, ⁴CNR-IOM Istituto Officina dei Materiali, Trieste, Italy

The ability to encode different operations into a single miniaturized optical device is required to reduce the complexity and size of optical paths for light manipulation, which usually employs dynamic optical components, interferometric setups, and/or multiple bulky elements in cascade. A very efficient solution is provided by metalenses, which are flat optical elements able to generate and manipulate structured light beams in a compact and efficient way, offering a powerful and attractive tool in many fields, such as life science and telecommunications. In this work, we present the design and test of transmission dielectric bi-functional metalenses that exploit both the dynamic and the geometric phases, to enable the spin-controlled manipulation of different focused orbital angular momentum (OAM) beams, depending on the circularly polarized state in input. In detail, we provide numerical algorithms for the design and simulation of the meta-optics in the telecom infrared, the fabrication processes, and the optical characterization under different impinging polarized optical vortices. This solution provides new integrated flat optics for applications in imaging, optical tweezing and trapping, optical computation, and high-capacity telecommunication and encryption.

KEYWORDS

metalens, meta-optics, flat optics, orbital angular momentum, structured light

1 Introduction

Allen and co-workers' seminal paper [1] paved the way for the research field of structured light, leading to scientific milestones and innovative applications in many areas, such as life science, information and communication technology, and quantum technologies [2–4]. In particular, wavefields carrying orbital angular momentum (OAM), so-called OAM beams or optical vortices (OVs), are endowed with peculiar ring-like intensity distributions and twisted wavefronts which revealed powerful applications in high-resolution microscopy [5], optical micro-manipulation [6–8], security [9], and light-matter interaction [10], while offering a new degree of freedom to encode information both in classical [11, 12] and single-photon regimes [13–15].

Spiral phase plates (SPPs) [16] represent one of the first stable, efficient, and compact optical elements proposed to generate structured light carrying orbital angular momentum from ordinary non-structured beams. These optics have 3D staircase profiles resembling the

twisted wavefront imparted to the impinging beam [17]. It is possible to generate high-purity and multi-ring OAM beams using SPPs with both azimuthal and radial discontinuities, to enable the excitation of higher-order modes by exploiting high-resolution lithographic techniques [18–20]. Nevertheless, spiral phase plates are limited to a single functionality. The advent of metasurfaces promoted the evolution of SPPs into the so-called q -plates [21] acting on the geometric phase to impart a polarization-dependent beam shaping [21]. Rather than shaping the wavefront by changing the local thickness of an isotropic material, i.e., the dynamic phase, in q -plates the thickness is fixed while the phase is manipulated by controlling the local anisotropy of the effective material. In particular, the imparted phase is equal to twice the local orientation of the extraordinary axis, and the sign is dependent on the handedness of the circular polarization in input. The first solutions relied on controlling the inherent anisotropy of liquid crystals [21–23], then artificial anisotropy was introduced by using properly oriented digital gratings [24, 25] or dielectric resonators [26, 27], so-called metaunits, to induce an effective form of birefringence. Metasurfaces represented a revolution in optics. Moving from 3D sculptured optics to 2D flat digital meta-optics exploiting silicon manufacturing has enabled the merging of optics and silicon photonics [28, 29]. Furthermore, the metasurface paradigm has included polarization as an additional degree of freedom for light structuring, extending the optical functionalities to enable the possibility of decoupling spin from phase reshaping and building up spin-dependent optical elements [30] [31]. One solution is offered by dual-functional metasurfaces [32–35], which act locally on both the dynamic and the geometric phases. That is achieved using anisotropic nanopillars, which have different tailored shapes to act on the dynamic phase and control their local fast-axis orientation to adjust the polarization-dependent geometric phase contribution.

In this work, we present the fabrication and optical characterization of dual-functional metalenses working in the telecom infrared, specifically designed for the generation of two distinct focused OAM beams, depending on the polarization state of the impinging light. In particular, we show that by switching the input polarization handedness, it is possible to select a spin-dependent OAM shift of the desired optical vortex in input at a specific position in space. This approach improves the functionality and integration level of standard spiral phase plates and q -plates, providing new advanced optical elements for applications to high-resolution microscopy, optical micro-manipulation, and classical and quantum information.

2 Material and methods

2.1 Dual-functional metalenses design

In this work, we propose a spin-dependent dielectric metasurface made of a squared lattice (period of the lattice $u = 600$ nm) of birefringent metaunits (MUs), so-called metaatoms (MAs), acting both on the geometric and dynamic phases. Each metaunit is represented by a crystalline silicon (c-Si) nanofin on a c-Si substrate. The cross-section of each metaunit is chosen within a library of 13 different nanostructures with different shapes and/or

orientations but the same height. In detail, as reported in our previous works [36], we find a set of rectangular-based, elliptical-based and pairs of different bevelled rectangular-based nanofins. At the same time, the height was optimized at 850 nm in order to cover the $0-2\pi$ dynamic phase range that is mandatory to satisfy the dual-functional paradigm. Since the metaunit size is below the diffraction limit, input light experiences an effective uniaxial medium with dynamic phase delays δ_x and δ_y , on the two axes, referring to TM and TE linear polarizations, respectively. All the nanostructures of the library act as half-wave plates (HWP) in order to maximize the polarization conversion and, therefore, the optical efficiency [37–39]. Then, a rotation by an angle θ of the anisotropic metaunit introduces a spin-dependent geometric phase equal to $\pm 2\theta$, depending on the handedness of the impinging circular polarization state, while the local dynamic phase depends on the metaunit cross-section. Thus, combining these two properties and selecting judiciously the metaunits pixel-by-pixel on the whole metasurface area, the metalens can behave differently depending on whether the input beam is right-handed (RCP) or left-handed circularly polarized (LCP).

The objective is that two circularly polarized beams with opposite handedness (i.e., RCP and LCP) experience different phase patterns ϕ^+ and ϕ^- , which are related to the dynamic and geometric phase according to the constitutive relations Eqs (1)–(3):

$$\delta_x = \frac{\phi^+(x, y) + \phi^-(x, y)}{2}, \quad (1)$$

$$\delta_y = \frac{\phi^+(x, y) + \phi^-(x, y)}{2} + \pi, \quad (2)$$

$$2\theta = \frac{\phi^+(x, y) - \phi^-(x, y)}{2}, \quad (3)$$

While the dynamic phase imparts the same contribution to both the RCP and LCP input beams, the geometric phase implies the transfer of symmetrical (opposite) phase delays for the two circularly polarized states, which combine to induce the desired spin-dependent phase modulation, that is:

$$J|L\rangle = -ie^{i(\delta_x + \delta_y)/2} e^{+i2\theta} |R\rangle = e^{i\phi^+} |R\rangle, \quad (4)$$

$$J|R\rangle = -ie^{i(\delta_x + \delta_y)/2} e^{-i2\theta} |L\rangle = e^{i\phi^-} |L\rangle. \quad (5)$$

J is the Jones matrix of the anisotropic metaatom [40, 41].

As well known, it is possible to describe a linearly polarized beam as the linear combination of a left-handed circularly polarized state ($|L\rangle$) and a right-handed circularly polarized one ($|R\rangle$). Thus, by illuminating the metasurface with a linearly polarized beam, it is possible to activate simultaneously the two functionalities designed for impinging circularly polarized light.

As we are interested in generating focused OAM beams, we need to properly design the local phase delay imparted by each metaunit in order to transfer the desired topological charge and focus the optical vortex onto two distinct points in space. To this aim, we encoded a converging lens profile ϕ :

$$\phi(r, \varphi) = \ell\varphi - k\left(\sqrt{f^2 + |\mathbf{r} - \mathbf{p}|^2} - f\right), \quad (6)$$

being ℓ the amount of OAM per photon (in units of \hbar) (or topological charge) transferred to the beam, $k = 2\pi/\lambda$ the wavevector, f the focal length, and $\mathbf{p} = (x_0, y_0)$ the focus

coordinates on the focal plane perpendicular to the propagation axis (z) and placed at a distance f [42–46].

To impart two different topological charges in two distinct positions, we can rewrite Eq. (6) using the notations of Eqs 4, 5:

$$\phi^\pm(r, \varphi) = \ell^\pm \varphi - k \left(\sqrt{f_\pm^2 + |r - \mathbf{p}|^2} - f_\pm \right), \quad (7)$$

where ℓ^\pm are the topological charges imparted to the impinging left-handed and right-handed circularly polarized beams respectively, while f_\pm represent the corresponding positions of the focal planes.

2.2 FEM simulations

The library of metaatoms was extrapolated by performing numerical simulations with Finite-Element Method (FEM) in the wavelength domain (COMSOL Multiphysics®). Each subunit was modelled as a silicon nanopillar ($n_{\text{Si}} = 3.5030$) surrounded by air ($n_{\text{Air}} = 1$) designed on the top of a silicon substrate ($n_{\text{Si}} = 3.5030$), and all the materials were considered as non-absorbing [$n = \text{Re}(n)$, $\text{Im}(n) = 0$]. Among all the possible configurations, a set of 13 pillars has been selected, covering the whole 2π range of dynamic phase and satisfying the conditions of half-wave plate and equal transmissions for TE and TM polarizations. Full details regarding metaunits shape and corresponding phase delays are reported in [36]. In detail, to ensure the HWP behaviour of each meta-unit, we selected metaatoms having a maximum phase difference of 0.03 rad from the HWP condition ($\delta_x - \delta_y < \pi \pm 0.03 \text{ rad}$), concurrently, we fixed $|T_{x,i} - T_{y,i}| \leq 0.05$, being $T_{x,i}$ and $T_{y,i}$ the transmittance of the i th metaatom for TE and TM polarizations, respectively, to ensure the validity of above Eqs 4, 5. Moreover, we imposed a maximum difference of 0.1 in transmittance among the 13 different metaatoms to guarantee a homogeneous transmittance over the whole metalens. We used custom MatLab scripts to transfer the maps of dynamic and geometric phases into a GDSII file encoding the cross-sections of the meta unit in each cell of the 2D metasurface lattice with period 600 nm in the x - and y -directions. Finally, the CAD file was uploaded to the software of the electron-beam lithographic system, and the design was materialized after exposure and development on the resist layer.

2.3 Fabrication

The designed metaoptics was fabricated via a two-step fabrication procedure. High-resolution electron beam lithography (EBL) was employed to transfer the optimized computational pattern onto a resist layer. In particular, a thin PMMA resist layer, deposited on a $\langle 100 \rangle$ silicon substrate, was patterned using an EBL system (Carl Zeiss Sigma 300, 30 keV beam voltage). Subsequently, a lift-off process was executed exploiting a thin mask of Al_2O_3 . Finally, the pattern was transferred onto the underlying silicon substrate through Inductively Coupled Plasma Reactive Ion Etching (ICP-RIE). ICP-RIE was performed in a STS Multiplex ASE using a mixture of $\text{SF}_6:\text{C}_4\text{F}_8:\text{Ar}$ (3:6:1). The plasma conditions and etching time were optimized in order to reach the optimal thickness and, thus, reduce the zero-order contribution [47, 48].

2.4 Optical characterization setup

The beam illuminating the metasurface was produced employing a Liquid Crystal on Silicon (LCoS) spatial light modulator (SLM) (X13267-08, Hamamatsu, pixel pitch $12.5 \mu\text{m}$) through a technique involving both phase and amplitude modulation. Collimation of the output from a DFB laser ($\lambda = 1310 \text{ nm}$, 1310LD34 1-2-2-1 CCSI, AeroDiode) at the termination of a single mode fiber was achieved using an aspheric lens with a focal length of 7.5 mm (A375TM-C, Thorlabs). The beam was then linearly polarized (LPIREA100-C, Thorlabs), expanded by a first telescope ($f_1 = 3.5 \text{ cm}$, $f_2 = 10.0 \text{ cm}$), and directed towards the display of the SLM for reshaping and/or optical vortex generation (Figure 1).

A 50:50 beam-splitter was positioned before the SLM, directing the reflected structured beam into the desired optical path and enabling an additional optical path for interferometric analysis. A 4- f system ($f_3 = 20.0 \text{ cm}$, $f_4 = 12.5 \text{ cm}$) was put in cascade with an aperture in the Fourier plane to isolate the first-order encoded mode and adjust the desired illuminating beam waist. In between, a quarter-wave plate (QWP) (WPQ10M-1310, Thorlabs) or a half-wave plate (HWP1) (WPH05M-1310, Thorlabs) were used to generate circularly polarized states from the original horizontally polarized one or rotate the polarization plane of the beam exiting the SLM, respectively. The polarized beam illuminated the meta-optics, mounted on a 6-axis kinematic mount (K6XS, Thorlabs). Finally, the OAM-shifted beam was collected using a $\times 10$ Objective (CFI E Plan Achromat $\times 10$, Nikon) positioned on a micrometric translator stage (LX20/M, Thorlabs). The image was captured by a CCD camera (WiDy SWIR 640U-S, pixel pitch $12.5 \mu\text{m}$). It was possible to generate an interferometric pattern using the additional optical arm, opening the iris (D2). The microscope objective was necessary to properly extract and magnify the generated beams since the focal lengths were too short to collect the beam directly on the CCD camera.

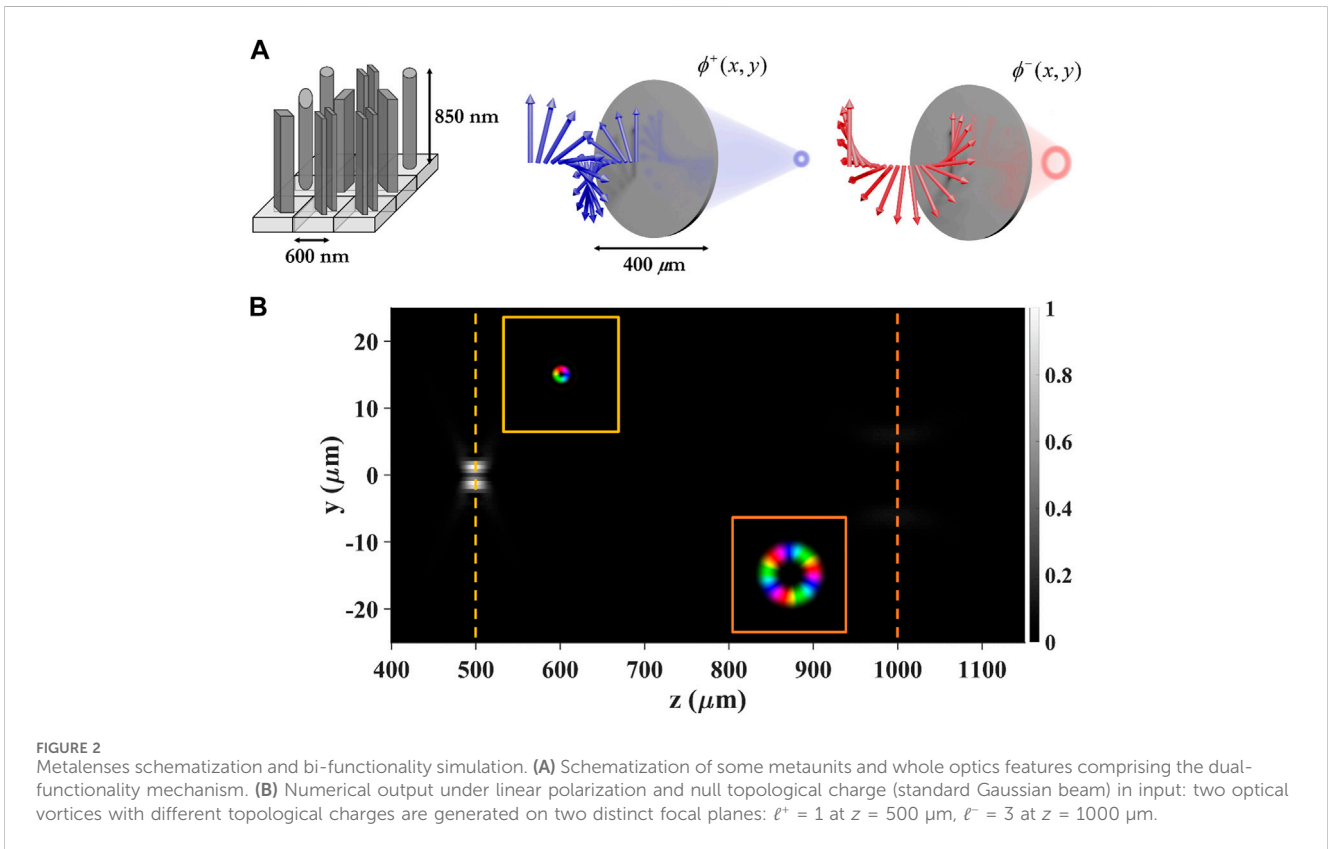
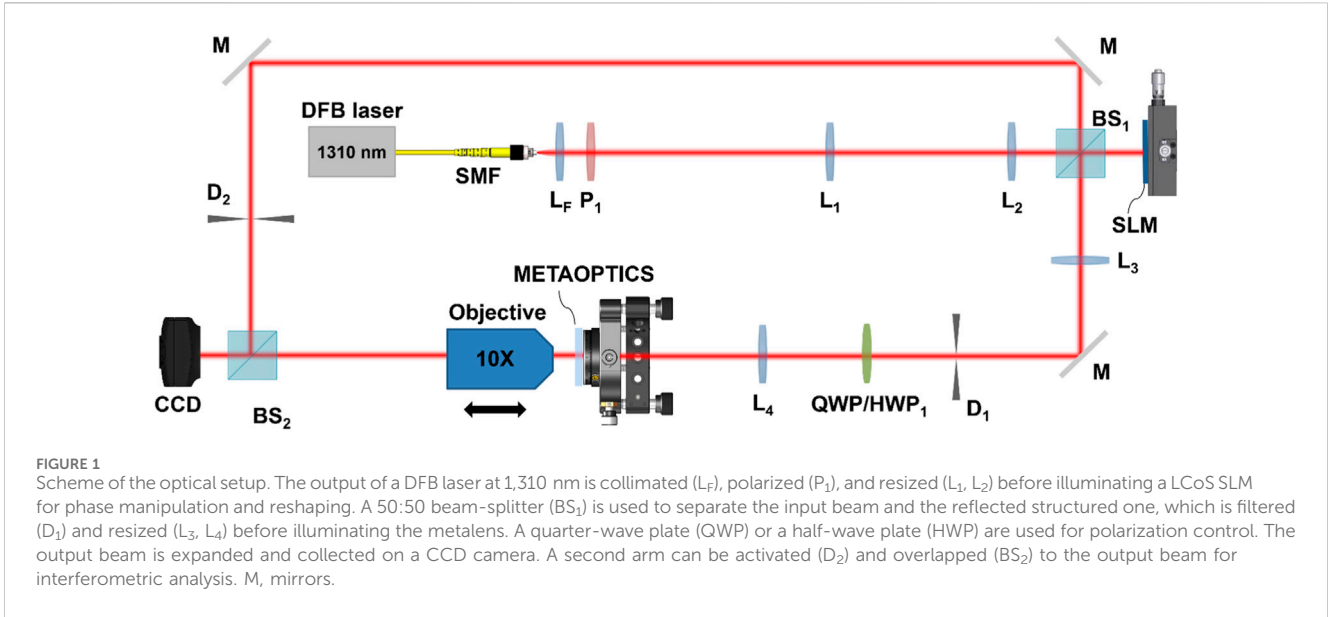
3 Results

Exploiting the dual-functional mechanism described in the previous section, we designed a spin-decoupled metalens which imparts two different topological charges $\ell^+ = 1$ and $\ell^- = 3$ to left-handed and right-handed circularly polarized light, and focuses the output beams at a distance of $f_+ = 500 \mu\text{m}$ and $f_- = 1000 \mu\text{m}$ from the optical element, respectively.

At first, we simulated the spin-decoupled behavior under the illumination of a Gaussian beam with a waist of $175 \mu\text{m}$. To test the two different polarization-dependent responses simultaneously, we chose a linearly polarized light in input.

Figure 2 depicts, as expected, the simultaneous generation of two distinct OAM beams with the desired topological charges at $500 \mu\text{m}$ and $1000 \mu\text{m}$. It is clear how the beam generated from the right-handed contribution has a larger waist and a lower intensity profile because it carries a higher topological charge and is focused on a plane placed at a larger distance.

Then, we simulated the behaviour of the metalens under the illumination of beams that already carry a topological charge (i.e., from -3 to 3). In particular, we modelled the impinging structured beam as a perfect vortex (PV) having a ring radius (ρ)



of $125 \mu\text{m}$ and a ring width ($d\rho$) of $50 \mu\text{m}$, as described by the equation Eq (8):

$$PV(r) = \exp\left(-\left(\frac{r-\rho_0}{d\rho_0}\right)^2\right). \tag{8}$$

Figure 3 presents the results we have obtained. In the first row (in blue), the phase and intensity pattern of the impinging perfect

vortex are reported. The second (yellow) and third (orange) rows report the generated structured beams under LCP and RCP illumination, respectively. Due to the half-wave plate behaviour, each metaatom reverses the handedness of the impinging light as reported in Eqs 4, 5, so the OAM beam focused at $500 \mu\text{m}$ is right-handed circularly polarized. Instead, the one generated at $1,000 \mu\text{m}$ is left-handed circularly polarized. As expected, we can see that the metalens acts as a dual-functional shifter of topological charge. In

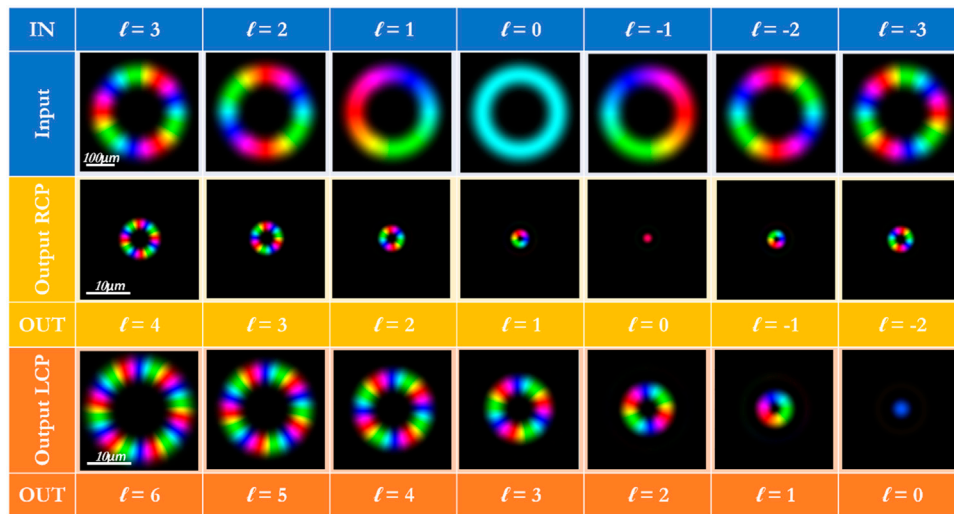


FIGURE 3 Numerical simulation under circularly polarized optical vortices in input. Numerical simulations of the metalens output when illuminated with circularly polarized perfect vortices of different topological charge in the range between $\ell = -3$ and $\ell = +3$. Depending on the handedness of the input beam, the optical vortex experiences polarization conversion and an OAM-shift equal to $+1$ or $+3$.

fact, the resulting generated beam carries a topological charge ℓ_{OUT} equal to the sum of the topological charge of the illuminating beam ℓ_{IN} with the spin-dependent topological charge ℓ^{\pm} imparted by the metalens. Moreover, the generated beams increase their waist with the resulting topological charge. As a matter of fact, in the far-field we collect the Fourier transform of a perfect vortex, which is well described by a Bessel-Gaussian beam. With respect to perfect vortices, the intensity profile of those beams is not OAM-independent, thus the radius of the inner intensity rings increases with the carried topological charge.

Subsequently, we numerically estimated the purity of the generated OAM modes by analyzing the OAM spectrum of the generated beam $U(\rho, \theta)$ at the focal plane using the expression Eq (9) [49]:

$$\eta_l = \frac{I_l}{I} = \frac{\int_0^{+\infty} |u_l(\rho)|^2 \rho d\rho}{\sum_{l=-\infty}^{+\infty} \int_0^{+\infty} |u_l(\rho)|^2 \rho d\rho}, \tag{9}$$

where $u_l(\rho) = \frac{1}{2\pi} \int_{-\pi}^{+\pi} U(\rho, \theta) \exp(-il\theta) d\theta$.

In Figure 4, we report the OAM spectrum analysis of the output beams under the illumination conditions mentioned above. The OAM shift of the output beams with respect to the input one confirms what expected from the metalens design. The generated OAM beams show no significant presence of spurious terms for the two outgoing circularly polarized beams. The spurious contributions are lower than 0.05 for all the different impinging configurations, proving that the conversion efficiency is very high.

Then, we fabricated the metasurface with a radius of $400 \mu\text{m}$ using the procedure described in Section 2.3.

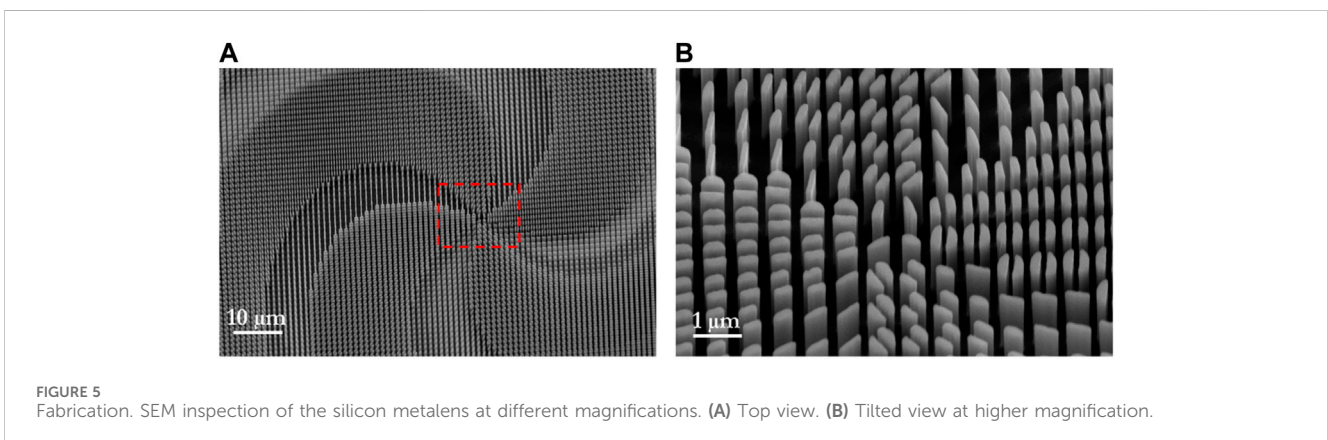
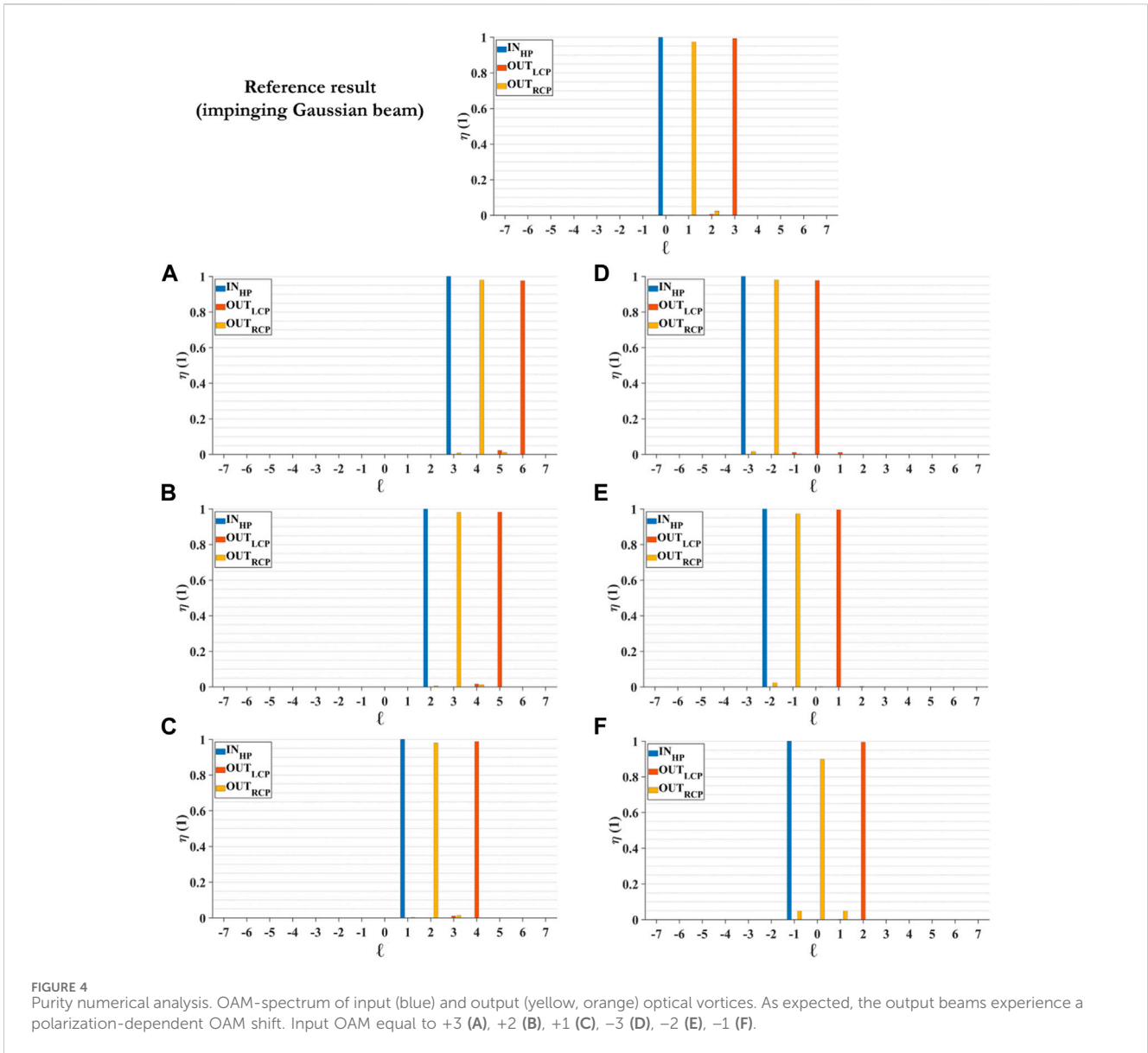
Figure 5 displays several SEM images of the fabricated silicon metasurface.

Finally, we optically characterized the performances of the designed metalens using the optical setup reported in Section 2.4. As expected, the two output beams present an intensity pattern that varies depending

on the impinging perfect vortex, suggesting an increase of the output orbital angular momentum, because of the interaction with the metalens (Figure 6B). To confirm this, we measured the interferogram pattern, which gave us information on the carried phase. It is clearly visible that the number of arms of the spiral, indicating the topological charge carried by the beam, are dictated by the sum of the impinging OAM plus the charge imparted by the metalens, which depends on the polarization state (Figure 6A).

4 Discussion and conclusion

This work presents the design, fabrication, and test of dual-functional silicon metalenses for the polarization-controlled manipulation of OAM beams. The optical element was designed to properly generate different non-overlapping focused beams carrying orbital angular momentum depending on the polarization state of the illuminating light. This optical behaviour is achieved by exploiting the dual-functional metalens capability to act on the dynamic and geometric phases simultaneously in order to introduce spin-dependent phase delays. The metaoptics has been fabricated using a two-step process: lithography of a resist mask with EBL and subsequent pattern transfer into the silicon substrate using ICP-RIE. Finally, we have characterized the optical response of the fabricated metalens to prove the effective polarization-dependent device as a topological charge shifter. The experimental results agree with the simulations, proving the design quality and the fabrication protocols optimization. While in this paper we present the generation of OAM beam, the method can be extended to the design of any metaoptics aimed to impart given phase patterns with high dimensionality or complex symmetry [50] to the different impinging circularly polarized states of light. In particular, we generated a single wavelength library, but by selecting more complicated coupled resonant metaunits, it is possible to achieve full achromaticity [51, 52]. Dual-functionality represents a tool that boosts the optical operations of



previous optical devices, such as diffractive elements or metasurfaces acting only on geometric or dynamic phases. This attractive solution can inspire advanced applications in imaging, microscopy, particle

manipulation, and quantum technologies, wherever tiny and compact multi-functional optical devices, fabricated using silicon technology manufacturing, are required.

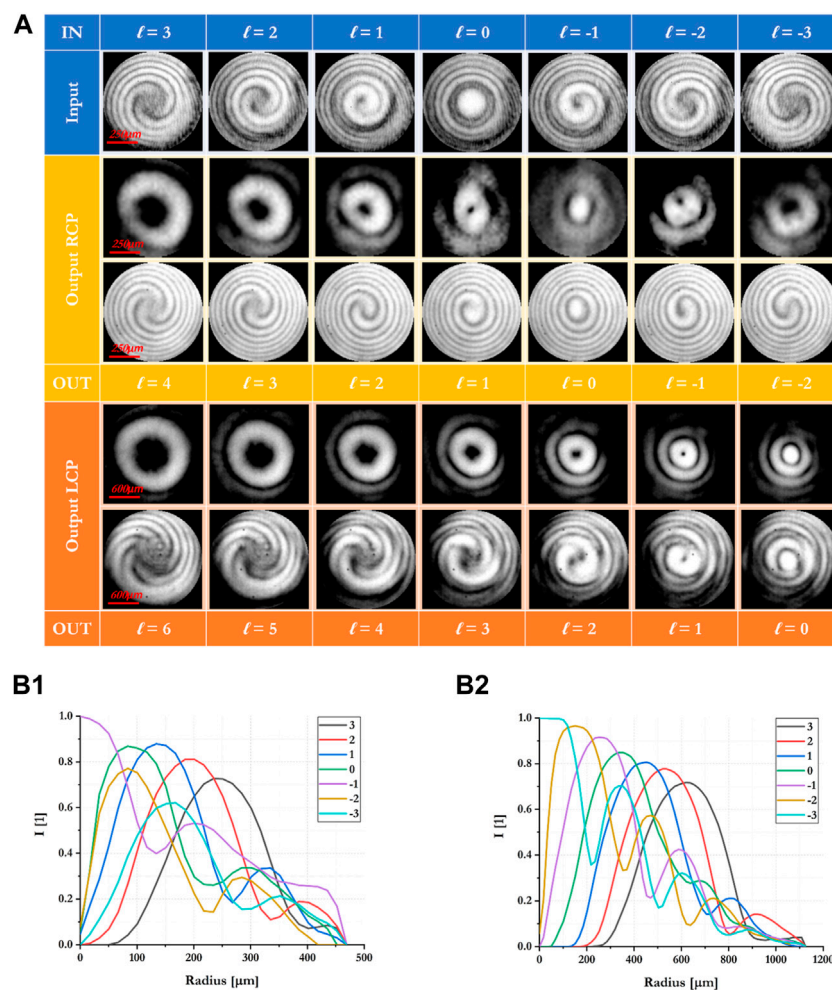


FIGURE 6 Experimental characterization and intensity radial profile. **(A)** Experimental analysis of the metalens output when illuminated with circularly-polarized perfect vortices of different topological charge in the range between $\ell = -3$ and $\ell = +3$. Depending on the handedness of the input beam, the optical vortex experiences an OAM-shift equal to $+1$ or $+3$ and polarization conversion, as expected. Counting the number of spiral arms in the interferograms it is possible to infer the carried OAM and prove the output OAM shift with respect to the input one. **(B)** Intensity radial profile for right-handed **(B1)** and left-handed **(B2)** circularly polarized optical vortices as a function of the input OAM.

Data availability statement

The raw data supporting the conclusion of this article will be made available by the authors, with under reasonable request.

Author contributions

AV: Conceptualization, Methodology, Software, Writing–original draft, Writing–review and editing. DB: Methodology, Writing–original draft, Writing–review and editing. SD: Methodology, Writing–original draft, Writing–review and editing. FR: Funding acquisition, Supervision, Writing–original draft, Writing–review and editing. GR: Funding acquisition, Supervision, Writing–original draft, Writing–review and editing, Methodology, Software.

Funding

The author(s) declare that financial support was received for the research, authorship, and/or publication of this article. This work was supported by the project STRADA (Italian Presidency of the Council of Ministers) and also partially supported by the European Union under the Italian National Recovery and Resilience Plan (NRRP) of NextGenerationEU, partnership on “Telecommunications of the Future” (PE0000001–program “RESTART”).

Conflict of interest

The authors declare that the research was conducted in the absence of any commercial or financial relationships that could be construed as a potential conflict of interest.

Publisher's note

All claims expressed in this article are solely those of the authors and do not necessarily represent those of their affiliated

organizations, or those of the publisher, the editors and the reviewers. Any product that may be evaluated in this article, or claim that may be made by its manufacturer, is not guaranteed or endorsed by the publisher.

References

- Allen L, Beijersbergen MW, Spreeuw RJC, Woerdman JP. Orbital angular momentum of light and the transformation of Laguerre-Gaussian laser modes. *Phys Rev A* (1992) 45:8185–9. doi:10.1103/physreva.45.8185
- Rubinsztein-Dunlop H, Forbes A, Berry MV, Dennis MR, Andrews DL, Mansuripur M, et al. Roadmap on structured light. *J Opt* (2016) 19:013001. doi:10.1088/2040-8978/19/1/013001
- Padgett MJ. Orbital angular momentum 25 years on [Invited]. *Opt Express* (2017) 25(10):11265–74. doi:10.1364/oe.25.1011265
- Shen Y, Wang X, Xie Z, Min C, Fu X, Liu Q, et al. Optical vortices 30 years on: OAM manipulation from topological charge to multiple singularities. *Light: Sci Appl* (2019) 8(1):90. doi:10.1038/s41377-019-0194-2
- Willig KI, Harke B, Medda R, Hell SW. STED microscopy with continuous wave beams. *Nat Methods* (2007) 4(11):915–8. doi:10.1038/nmeth1108
- Padgett M, Bowman R. Tweezers with a twist. *Nat Photon* (2011) 5(6):343–8. doi:10.1038/nphoton.2011.81
- Tian Y, Wang L, Duan G, Yu L. Multi-trap optical tweezers based on composite vortex beams. *Opt Commun* (2021) 485:126712. doi:10.1016/j.optcom.2020.126712
- MacDonald MP, Paterson L, Volke-Sepulveda K, Arlt J, Sibbett W, Dholakia K. Creation and manipulation of three-dimensional optically trapped structures. *Science* (2002) 296(5570):1101–3. doi:10.1126/science.1069571
- Zhang F, Guo Y, Pu M, Chen L, Xu M, Liao M, et al. Meta-optics empowered vector visual cryptography for high security and rapid decryption. *Nat Commun* (2023) 14(1):1946. doi:10.1038/s41467-023-37510-z
- Lembessis VE, Babiker M. Enhanced quadrupole effects for atoms in optical vortices. *Phys Rev Lett* (2013) 110(8):083002. doi:10.1103/physrevlett.110.083002
- Wang J. Twisted optical communications using orbital angular momentum. *China Phys Mech Astron* (2019) 62(3):34201. doi:10.1007/s11433-018-9260-8
- Wan Z, Wang H, Liu Q, Fu X, Shen Y. Ultra-degree-of-freedom structured light for ultracapacity information carriers. *ACS Photon* (2023) 10(7):2149–64. doi:10.1021/acsp Photonics.2c01640
- Sit A, Bouchard F, Fickler R, Gagnon-Bischoff J, Larocque H, Heshami K, et al. High-dimensional intracity quantum secret sharing with structured photons. *Optica* (2017) 4(9):1006–10. doi:10.1364/optica.4.001006
- He C, Shen Y, Forbes A. Towards higher-dimensional structured light. *Light: Sci Appl* (2022) 11(1):205. doi:10.1038/s41377-022-00897-3
- De Oliveira M, Nape I, Pinnell J, TabeBordbar N, Forbes A. Experimental high-dimensional quantum secret sharing with spin-orbit-structured photons. *Phys Rev A* (2020) 380 101(4):042303. doi:10.1103/physreva.101.042303
- Khonina SN, Kotlyar VV, Shinkaryev MV, Soifer VA, Uspleniev GV. The phase rotor filter. *J Mod Opt* (1992) 39:1147–54. doi:10.1080/09500349214551151
- Turnbull GA, Robertson DA, Smith GM, Allen L, Padgett MJ. The generation of free-space Laguerre-Gaussian modes at millimetre-wave frequencies by use of a spiral phase plate. *Opt Commun* (1996) 127:183–8. doi:10.1016/0030-4018(96)00070-3
- Massari M, Ruffato G, Gintoli M, Ricci F, Romanato F. Fabrication and characterization of high-quality spiral phase plates for optical applications. *Appl Opt* (2015) 54(13):409 4077–83. doi:10.1364/ao.54.004077
- Ruffato G, Massari M, Romanato F. Generation of high-order Laguerre-Gaussian modes by means of spiral phase plates. *Opt Lett* (2014) 39(17):5094–7. doi:10.1364/ol.39.005094
- Ruffato G, Massari M, Carli M, Romanato F. Spiral phase plates with radial discontinuities for the generation of multiring orbital angular momentum beams: fabrication, characterization, and application. *Opt Eng* (2015) 54(11):111307. doi:10.1117/1.oe.54.11.111307
- Marrucci L, Manzo C, Paparo D. Optical spin-to-orbital angular momentum conversion in inhomogeneous anisotropic media. *Phys Rev Lett* (2006) 96:163905. doi:10.1103/physrevlett.96.163905
- Brasselet E. Tunable high-resolution macroscopic self-engineered geometric phase optical elements. *Phys Rev Lett* (2018) 121(3):033901. doi:10.1103/physrevlett.121.033901
- Ruffato G, Brasselet E, Massari M, Romanato F. Electrically activated spin-controlled orbital angular momentum multiplexer. *Appl Phys Lett* (2018) 113(1):011109. doi:10.1063/1.5030844
- Desiatov B, Mazurski N, Fainman Y, Levy U. Polarization selective beam shaping using nanoscale dielectric metasurfaces. *Opt Express* (2015) 23(17):22611–8. doi:10.1364/oe.23.022611
- Ruffato G, Romanato F. Design of continuously variant metasurfaces for conformal transformation optics. *Opt Express* (2020) 28(23):34201–18. doi:10.1364/oe.400627
- Devlin RC, Ambrosio A, Wintz D, Oscurato SL, Zhu AY, Khorasaninejad M, et al. Spin-to-orbital angular momentum conversion in dielectric metasurfaces. *Opt Express* (2017) 25(1):377–93. doi:10.1364/oe.25.000377
- Chen MH, Liu YL, Su VC. Gallium nitride-based geometric and propagation metasurfaces for vortex beam emissions. *Heliyon* (2024) 10(3):e25436. doi:10.1016/j.heliyon.2024.e25436
- Genevet P, Capasso F, Aieta F, Khorasaninejad M, Devlin R. Recent advances in planar optics: from plasmonic to dielectric metasurfaces. *Optica* (2017) 4:139–52. doi:10.1364/optica.4.000139
- Capasso F. The future and promise of flat optics: a personal perspective. *Nanophotonics* (2018) 7(6):953–7. doi:10.1515/nanoph-2018-0004
- Devlin RC, Ambrosio A, Rubin NA, Mueller JPB, Capasso F. Arbitrary spin-to-orbital angular momentum conversion of light. *Science* (2017) 358(6365):896–901. doi:10.1126/science.aao5392
- Huo P, Zhang C, Zhu W, Liu M, Zhang S, Zhang S, et al. Photonic spin-multiplexing metasurface for switchable spiral phase contrast imaging. *Nano Lett* (2020) 20(4):2791–8. doi:10.1021/acs.nanolett.0c00471
- Li S, Li X, Zhang L, Wang G, Zhang L, Liu M, et al. Efficient optical angular momentum manipulation for compact multiplexing and demultiplexing using a dielectric metasurface. *Adv Opt Mater* (2020) 8(8), 1901666. doi:10.1002/adom.201901666
- Guo Y, Zhang S, Pu M, He Q, Jin J, Xu M, et al. Spin-decoupled metasurface for simultaneous detection of spin and orbital angular momenta via momentum transformation. *Light: Sci Appl* (2021) 10(1):63–1. doi:10.1038/s41377-021-00497-7
- Su VC, Chiang CH, Chen MH, Xu KL, Huang SY. Metasurface-based perfect vortex beam for optical eraser. *Commun Phys* (2024) 7(1):36. doi:10.1038/s42005-024-01525-9
- Zhao H, Wang X, Liu S, Zhang Y. Highly efficient vectorial field manipulation using a transmitted tri-layer metasurface in the terahertz band. *Opto-Electronic Adv* (2023) 6(2):220012–1. doi:10.29026/oea.2023.220012
- Vogliardi A, Ruffato G, Dal Zilio S, Bonaldo D, Romanato F. Dual-functional metalenses for the polarization-controlled generation of focalized vector beams in the telecom infrared. *Sci Rep* (2023) 13(1):10327. doi:10.1038/s41598-023-36865-z
- Lin D, Fan P, Hasman E, Brongersma ML. Dielectric gradient metasurface optical elements. *Science* (2014) 345(6194):298–302. doi:10.1126/science.1253213
- Khorasaninejad M, Crozier KB. Silicon nanofin grating as a miniature chirality-distinguishing beam-splitter. *Nat Comm*. (2014) 5(1):5386–6. doi:10.1038/ncomms6386
- Zheng G, Mühlenbernd H, Kenney M, Li G, Zentgraf T, Zhang S. Metasurface holograms reaching 80% efficiency. *Nat Nanotech* (2015) 10(4):308–12. doi:10.1038/nnano.2015.2
- Vogliardi A, Romanato F, Ruffato G. Design of dual-functional metaoptics for the spin-controlled generation of orbital angular momentum beams. *Front Phys* (2022) 10:586. doi:10.3389/fphy.2022.870770
- Zhang K, Yuan Y, Ding X, Ratni B, Burokur SN, Wu Q. High-efficiency metalenses with switchable functionalities in microwave region. *ACS Appl Mater Inter* (2019) 11(31):28423–30. doi:10.1021/acsami.9b07102
- Andrews DL, Babiker M. *The angular momentum of light*. Cambridge University Press (2012).
- Su VC, Huang SY, Chen MH, Chiang CH, Xu KL. Optical metasurfaces for tunable vortex beams. *Adv Opt Mater* (2023) 11(24):2301841. doi:10.1002/adom.202301841
- Aieta F, Genevet P, Kats M, Capasso F. Aberrations of flat lenses and aplanatic metasurfaces. *Opt Express* (2013) 21(25):31530–9. doi:10.1364/oe.21.031530
- Aieta F, Genevet P, Kats MA, Yu N, Blanchard R, Gaburro Z, et al. Aberration-free ultrathin flat lenses and axicons at telecom wavelengths

based on plasmonic metasurfaces. *Nano Lett* (2012) 12(9):4932–6. doi:10.1021/nl302516v

46. Goodman JW. *Introduction to fourier optics*. Greenwood Village: Roberts & Co. Publishers (2005).

47. Vogliardi A, Ruffato G, Bonaldo D, Dal Zilio S, Romanato F. Silicon metaoptics for the compact generation of perfect vector beams in the telecom infrared. *Opt Lett* (2023) 48(18):4925–8. doi:10.1364/ol.501239

48. Vogliardi A, Ruffato G, Bonaldo D, Dal Zilio S, Romanato F. All-dielectric metaoptics for the compact generation of double-ring perfect vector beams. *Nanophotonics* (2023) 12(22):4215–28. doi:10.1515/nanoph-2023-0555

49. Ruffato G, Massari M, Romanato F. Multiplication and division of the orbital angular momentum of light with diffractive transformation optics. *Light: Sci Appl* (2019) 8(1):113. doi:10.1038/s41377-019-0222-2

50. Shen Y. Rays, waves, SU (2) symmetry and geometry: toolkits for structured light. *J Opt* (2021) 23(12):124004. doi:10.1088/2040-8986/ac3676

51. Chen WT, Zhu AY, Capasso F. Flat optics with dispersion-engineered metasurfaces. *Nat Rev Mater* (2020) 5:604–20. doi:10.1038/s41578-020-0203-3

52. Chen WT, Zhu AY, Sanjeev V, Khorasaninejad M, Shi Z, Lee E, et al. A broadband achromatic metalens for focusing and imaging in the visible. *Nat Nanotech* (2018) 13:220–6. doi:10.1038/s41565-017-0034-6